

# Manufacturing and Impact Behavior of Syntactic Foam

HO SUNG KIM, HOCK HUAT OH

Department of Mechanical Engineering, The University of Newcastle, Callaghan, NSW 2308, Australia

Received 11 May 1999; accepted 19 September 1999

**ABSTRACT:** Syntactic foam made of glass hollow microspheres and epoxy vinyl ester resin is manufactured by using a new manufacturing method and its impact behavior is studied in terms of protection parameters. Experimental results for impact force and stress as functions of specimen diameter were found to be in reasonable agreement with predictions based on a model. Also, some compression properties of the foam were investigated. It was found that there is similarity in compressive failure mode between pseudostatic and impact loadings. © 2000 John Wiley & Sons, Inc. *J Appl Polym Sci* 76: 1324–1328, 2000

**Key words:** syntactic foam; impact; compression; protection; hollow microsphere

## INTRODUCTION

Syntactic foams have been used in such areas where low densities are required as undersea/marine equipment for deep ocean current metering, antisubmarine warfare,<sup>1–5</sup> sandwich composites,<sup>6,7</sup> and others.<sup>8</sup> Also, their applications include products in aerospace and automotive industries.<sup>8</sup>

The manufacturing process of syntactic foams is different from that of conventional foams. The main porosity of the syntactic foams comes from preformed hollow microspheres. Some consolidating methods for binder and microspheres include coating microspheres<sup>9</sup> and using inorganic binder solution and firing,<sup>10</sup> dry resin powder,<sup>11–14</sup> and liquid resin.<sup>15</sup> The first method (coating) needs vacuum filtering and rinsing. All the other methods require heating for various reasons. The last method using liquid resin would be convenient and economical if practicable at room temperature.

The literature on syntactic foam for impact is sparse despite its great potential for impact ap-

plications. Some considerations in the past include impact fatigue<sup>16</sup> and postimpact damage.<sup>17,18</sup> However, impact behavior in terms of protection has scarcely been considered.

In this article, it is attempted to manufacture a particular syntactic foam using a new procedure. Also, since major design considerations for protection devices include impact force and impact stress,<sup>19–22</sup> the purpose of the work was to investigate the impact behavior of the syntactic foam in terms of protection parameters.

## EXPERIMENTAL

### Materials, Blending, and Specimens Preparation

For manufacturing of syntactic foam, hollow microspheres and Derakane 441-400 epoxy vinyl ester resin with a density of 1.07 (Dow Plastics, Midland, MI) was used as filler and matrix, respectively. The hollow microspheres used are Q-Cel 520 manufactured by PQ Australia Pty. Ltd., Dandenong, Vic., Australia. For size measurements, the microspheres Malvern 2600C laser particle size analyzer was used. The mean size of the spheres was found to be 40.16  $\mu\text{m}$  and 90% of the samples in a range of 17–82  $\mu\text{m}$ . For curing of the resin, methyl ethyl ketone peroxide

Correspondence to: H. S. Kim (mehsk@cc.newcastle.edu.au).

*Journal of Applied Polymer Science*, Vol. 76, 1324–1328 (2000)  
© 2000 John Wiley & Sons, Inc.

**Table I** Composition of Vinyl Ester/Q-Cel Foam

Material	Parts by Volume
Derakane 441-400	100
MEKP	2
CoNap	0.2
Q-Cel 520	39

(MEKP) and CoNap were added into the resin. Then, hollow microspheres were progressively added to the resin system while stirring the mixture gently and using a spatula by providing a shearing action in a mixing pot. The composition of the mixture is given in Table I. The particle and bulk densities of spheres were measured using a pycnometer (Model 930, Bechman) and found to be 0.22 and 0.13, respectively. The bulk density was initially time-dependent because of particle settling time so that the measurement was conducted 30 min after placing hollow microspheres in a measuring cylinder.

The mixture was charged into a cylindrical mold with a diameter of 28 mm and then it was compacted in a press at a pressure of 0.368 MPa. This was immediately followed by demolding. The compacting pressure was chosen by noting that commercial glass microspheres have about a 50% chance of surviving at a hydrostatic stress of 10.79 MPa.<sup>23</sup> The molding was machined into cylindrical specimens with a height of 20 mm but various diameters ranging 5, 10, 15, 17.5, and 20 mm. Densities of specimens were found to be 0.76. A manufactured specimen was broken with a hammer and a typical fracture surface for the microstructure is shown in Figure 1. Also, specimens of resin only without inclusion of microspheres were made for comparative use.

### Mechanical Testing

Compression testing was conducted on a universal testing machine (Shimadzu DSS 5000) at a crosshead speed of 5 mm/min for each diameter. Graphite fine powder (LC, APS Chemicals, 2459-500G) was applied to each specimen to reduce friction in the contact area between specimen and platens. A typical compressive stress-strain curve is given in Figure 2 to show a slope selected for the compressive modulus and a point at which fracture occurred.

Impact testing setup consisting of flat-ended impactors, load transducer, and data logging sys-

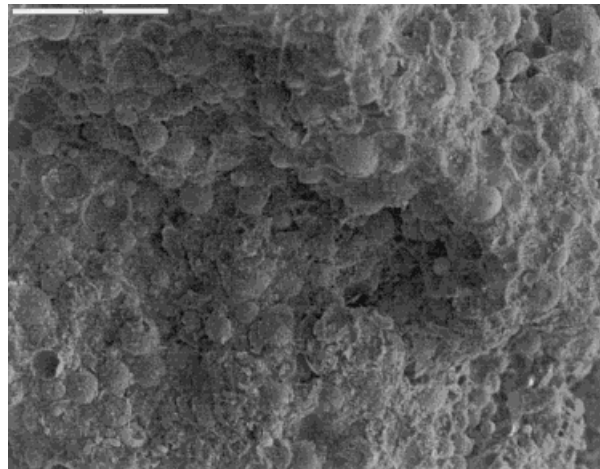


**Figure 1** Fracture surface revealing microstructure of vinyl ester/Q-Cel foam. The scale bar represents 200  $\mu\text{m}$ .

tem is schematically shown in Figure 3. It consists of a flat-ended impactor, an electromagnet for the impactor-release mechanism, a load cell with a capacity of 10 kN, and a computer with software for data logging (DocuWave, Version 1.10, Tektronix, Inc.). Two different impact energy levels were employed viz. 1.14 and 2.04 J using impactors weighing 171 and 306 g, respec-

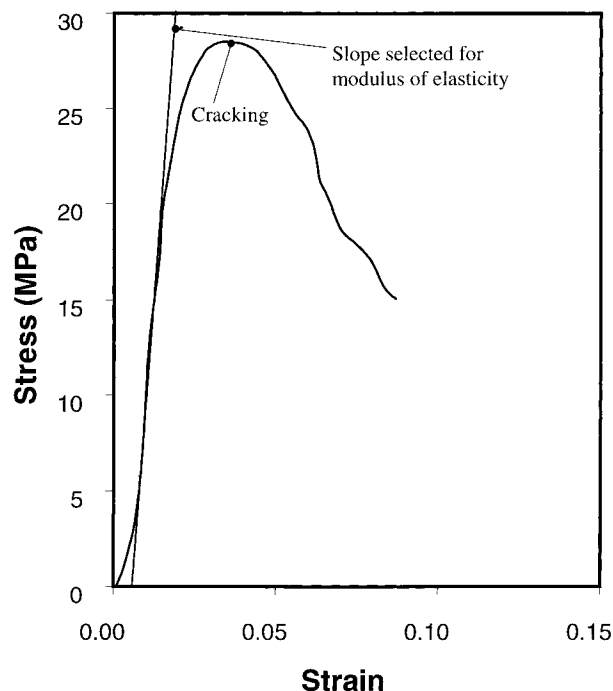


**Figure 2** Compression stress-strain curve obtained from a foam specimen with a diameter of 15 mm.

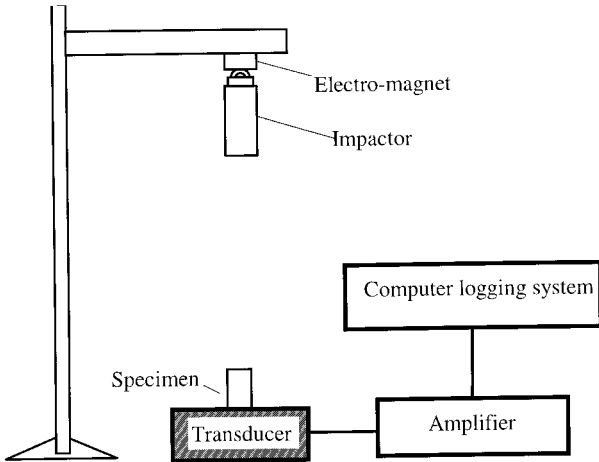


**Figure 3** Schematic impact test setup.

tively, but a constant impact height of 780 mm was kept.

## RESULTS AND DISCUSSION

As noted in Figure 2, the compressive stress-strain curve is somewhat different from that of conventional foam in which a plateau regime is part of the curve as a result of buckling of cell walls.<sup>24</sup> The curve in Figure 2 indicates that the hollow microspheres of the current syntactic foam did not get crushed prior to the peak stress. Compressive test results for foam and resin are listed in Table II. Compressive moduli of the foam with specimen diameters ranging from 5 to 17.5 mm appear to be generally low compared to that of resin, although a specimen with a diameter of 20 mm is higher than that of resin. The 20-mm increase of specimen in modulus seems to be due to

**Table II** Compressive Properties of Resin and Foam

Specimen Diameter (mm)	Compressive Modulus (GPa)	Strength (MPa)
5.0 (Pure resin)	4.20	—
5.0	2.40	22.50
10.0	2.33	22.28
15.0	2.43	25.44
17.5	3.33	22.60
20.0	5.95	29.52

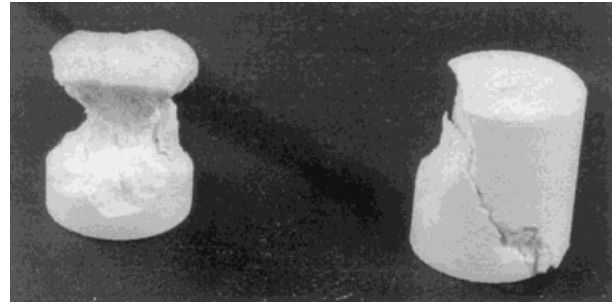


**Figure 4** Broken specimens under compression showing approximately 45° shear planes of fracture surfaces.

specimen-size effect because the influence of friction would increase with increasing diameter.<sup>25</sup> Not surprisingly, for the same reason, the strength of specimen with a diameter of 20 mm is high compared to those of any other foam specimens.

A typical failure mode of foam under compression is shown in Figure 4. This suggests that the failure is by shear on planes inclined approximately 45° to the loading direction and thus by fracture mode II. Fracture surface of a shear plane is also shown in Figure 5. Broken spheres are seen with debris. It is difficult, however, to find tunneling<sup>26</sup> or any other sign of fracture mode II,<sup>27,28</sup> but partially broken spheres seem to represent two-dimensional surface characteristics. The fracture-surface characteristics appear to be in contrast with one that was manufactured

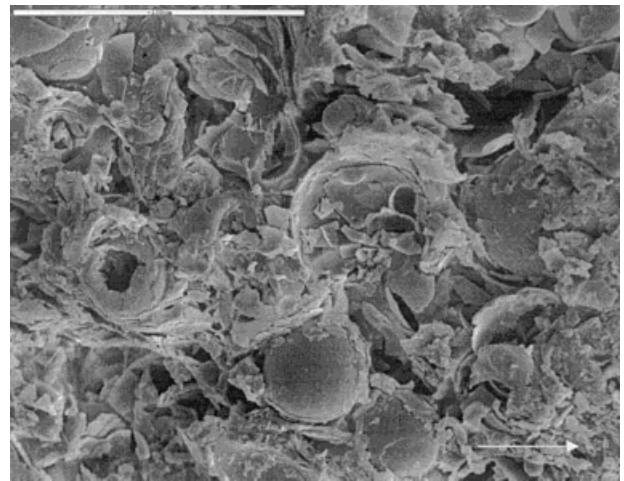


**Figure 5** Fracture surface of compressive specimen (Fig. 1) revealing broken spheres with debris. The scale bar represents 100  $\mu\text{m}$ . The arrow indicates the shear direction of the opposite plane.

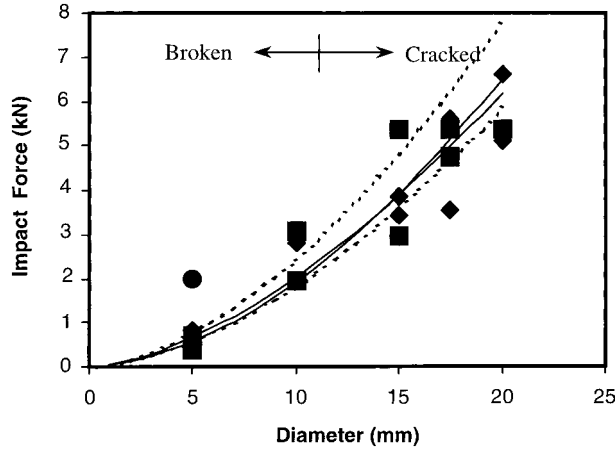


**Figure 6** Impact force as a function of specimen diameter: ●, resin (2.04 J); ◆, foam (1.14 J); and ■, foam (2.04 J); —, best fit line; and ···, predicted by eq. (1).

by coating spheres and its failure mechanisms are mainly by structural disintegration for low-resin content foams.<sup>9</sup>

The maximum impact force measured as a function of specimen diameter is given in Figure 6. The symbol ● represents pure resin at an impact-energy level of 2.04 J. The other two symbols ◆ and ■ represent foam at impact-energy levels of 1.14 and 2.04 J, respectively. The impact force (maximum peak) for resin appears to be much higher than those of foam for a diameter of 5 mm. This indicates that the inclusion of hollow microspheres in the resin is beneficial in reducing the impact force. Furthermore, the two solid lines represent the best fit curves (converted from log–log scales) for two different impact energy levels for foam as a function of specimen diameter. They show that there is not much difference in the impact force for the different energy levels. They also show some degree of nonlinearity. Judging from the reasonable linearity of stress–strain curve to the peak where fracture occurs (see Fig. 2), the nonlinearity here would be due to the strain-rate effect caused by specimen diameter variation.<sup>20–22</sup> This allows the use of a model for analysis represented by the following equation<sup>20–22</sup>:

$$F = d^m k \sqrt{\Lambda} \tag{1}$$

where  $F$  is the maximum impact force,  $d$  is the diameter,  $\Lambda$  is the impact energy, and  $(m, k)$  are constants. The obtained values for the constants are given in Table III. The predictions by eq. (1) is also given as dotted lines in Figure 6. It is seen that the prediction appears to be reasonable and there is not much difference between the two energy levels, although the difference in prediction is obvious compared to that in the experiment.

Average impact stresses obtained by converting the data are shown in Figure 7. Stress levels for foam and pure resin both with a diameter of 5 mm are easily distinctive with each other. However, the stress for foam does not appear to vary as much as the impact force over the range of diameters. The solid lines represent the best-fit curves (converted from log–log scales) of data points for foam at impact energy levels of 1.14 and 2.04 J. The difference in stress between two different impact energy levels is noticeable compared to that in the force shown in Figure 6. Predictions are made and given as dotted lines in Figure 7 using the following equation<sup>20–22</sup>:

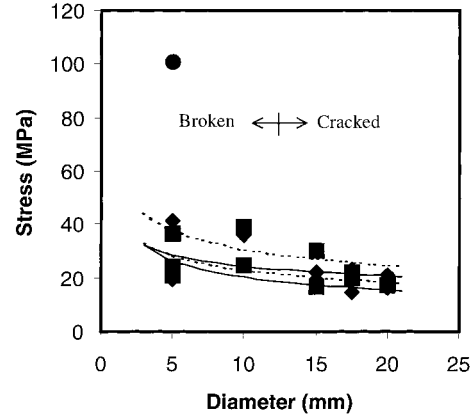


**Figure 7** Average impact stress as a function of specimen diameter: ●, resin (2.04 J); ◆, foam (1.14 J); ■, foam (2.04 J); —, best fit line; and ···, predicted by eq. (2).

**Table III** Constants for Foam in  $F = d^m k \sqrt{\Lambda}$  and  $\sigma = d^{m-2} k' \sqrt{\Lambda}$

Impact Energy (J)	$m$	$k$	$k'$	Mean $m$	Mean $k$	Mean $k'$
1.14	1.61	46.39	59.23			
2.04	1.77	22.63	28.76	1.69	22.63	44.00



$$\sigma = d^{m-2}k' \sqrt{\Lambda} \quad (2)$$

where  $\sigma$  is the stress and  $k'$  is a material constant. The obtained constants are listed in Table III. The prediction becomes favorable for large diameters.

It should be noted that the model has some limitations. For example, it does not consider the force ( $F$ ) of postfracture that may be affected by kinetic energy due to fracture. The smaller the diameter, the more the kinetic effect is expected. A posttest examination of impact specimens was conducted that divided the specimens into two groups: one is for broken specimens that may carry some kinetic energy during fracture and the other is for those with just visible cracks. The transitional point between the two groups is indicated in Figures 6 and 7. The cracking mode of the foam under impact loading had been found to be similar to that under pseudostatic compressive loading.

## CONCLUSIONS

Compression and impact behaviors of a syntactic foam manufactured by compaction have been studied. Compressive modulus of the foam was found to be reduced by a factor of 2 from that of resin for the same size specimens. Experimental results for impact force and stress were found to be in reasonable agreement with predictions. Also, it was demonstrated that inclusion of glass hollow microspheres in resin reduces impact force/stress.

## REFERENCES

1. Jackson, D.; Clay, P. *Sea Technol* 1983, 24, 29.
2. Harruff, P. W.; Sandman, B. E. in *Carbon/Epoxy Composite Structures for Underwater Pressure Hull Applications*; 28<sup>th</sup> National SAMPE Symposium, Anaheim, CA, April 12–14, 1983, pp 40–49.
3. Watkins, L. Syntactic foam buoyancy for production risers, Presented at the Seventh International Conference on Offshore Mechanical and Arctic Engineering, Houston, TX, Feb 7–12, 1988, p 403.
4. Seamark, M. J. *Cellul Polym* 1991, 10, 308.
5. Hinves, J. B.; Douglas, C. D. *IEEE*, in *Proceedings of the Conference on Ocean '93*, Part 3 (of 3), Victoria, BC, Canada, Oct 18–21, 1993, III-468–472.
6. ASTM STP 1274, *Annu Book ASTM Stand* 1996, pp 125–138.
7. English, L. K. *Mater Eng* 1987, 4, 51.
8. Young, K. S. *Mod Plast* April 1985; p 92.
9. Narkis, M.; Gerchovich, M.; Puterman, M.; Kenig, S. *J Cell Plast* 1982, July/August, 230.
10. Verweij, H.; De With, G.; Veeneman, D. *J Mater Sci* 1985, 20, 1069.
11. Puterman, M.; Narkis, M. *J Cellul Plast* 1980, July/August, 223.
12. Narkis, M.; Kenig, S. *J Cellul Plast* 1980, Nov/Dec, 326.
13. Kenig, S.; Raiter, I.; Narkis, M. *J Cellul Plast* 1984, Nov/Dec, 423.
14. Meter, C. *Int Pat B29C 65/00, B29D 9/00, B32B 3/26, 5/18*, 1997.
15. te Nijenhuis, K.; Addink, R.; van der Vegt, A. K. *Polym Bull* 1989, 21, 467.
16. Cohen, A.; Yalvac, S.; Wetters, D. G. in *Impact Behavior of a Syntactic Composite Material*; 37<sup>th</sup> International SAMPE Symposium, Anaheim, CA, March 9–12, 1992; p 641.
17. Hiel, C.; Ishai, O. in *Low- and High-Velocity Impact Response of Sandwich Panels with Syntactic Foam Core*, PVP-Vol. 225/NE-Vol. 7; *Recent Advances in Structural Mechanics*, ASME: Atlanta, GA, 1991; p 137.
18. Hiel, C.; Dittman, D.; Ishai, O. *Composites* 1993, 24, 447.
19. Kim, H. S.; Mathieu, K. *J Mat Sci: Mater Med* 1998, 9, 457.
20. Kim, H. S.; Stojcevski, S. *Impact Test with Flat-Ended Impactor for Mouthguard Materials Specimen Size Effect*, Society of Plastics Engineers, 56th Annual Technical Conference, ANTEC '98, Atlanta, GA, April 26–May 1, 1998, Vol. 3, Part 3, p 2738.
21. Kim, H. S. *Impact Test with Spherical Impactor for Mouthguard Materials: Specimen Size Effect*, in *CD Proceedings of ICTACEM98, International Conference on Theoretical, Applied, Computational and Experimental Mechanics*, Indian Institute of Technology, Kharagpur, India, December 1–5, 1998; Paper J07.
22. Kim, H. S.; Stojcevski, S. *J Reinforced Plast Compos* 1999, 18, 539.
23. Puterman, M.; Narkis, M.; Kenig, S. *J Cellul Plast* 1980, July/August, 223.
24. Neilsen, M. K.; Krieg, R. D.; Schreyer, H. L. *Polym Eng Sci* 1995, 35, 387.
25. Dieter, G. E. *Mechanical Metallurgy*; McGraw-Hill: New York, 1961; p 544.
26. Kim, H. S.; Ma, P. *J Appl Polym Sci* 1998, 69, 405.
27. Kim, H. S.; Ma, P. *Key Eng Mater* 1998, 137, 123.
28. Kim, H. S.; Ma, P. *Key Eng Mater* 1998, 145–149, 759.